



# <sup>18</sup>F-FDG PET/CT Parameters and Standard Uptake Values Predicting Contralateral Lung Metastasis in Lung Cancer

Akciğer Kanserinde Karşı Akciğer Parankim Metastazını Öngörmeye Yarayan <sup>18</sup>F-FDG PET/CT Parametreleri

✉ Büşra Özdemir Günay<sup>1</sup>, ✉ Funda Üstün<sup>2</sup>

<sup>1</sup>Giresun Training and Research Hospital, Clinic of Nuclear Medicine, Giresun, Türkiye

<sup>2</sup>Trakya University Faculty of Medicine, Department of Nuclear Medicine, Edirne, Türkiye

## Abstract

**Objectives:** Contralateral lung parenchymal metastasis (CLM), less common than expected in lung cancer, and its exact mechanism is still unknown. To determine the additional value of <sup>18</sup>F-fluorodeoxyglucose positron emission tomography/computed tomography (<sup>18</sup>F-FDG PET/CT) in determining CLM, its causes, and predictive factors in lung cancer.

**Methods:** The data were evaluated by comparing the group with CLM and the group without CLM but with distant metastasis to other organs, two groups known as the M1 classification according to the 9<sup>th</sup> tumor-node-metastasis classification in lung cancer. Histopathological data, follow-up, and <sup>18</sup>F-FDG PET/CT findings, including primary tumor lobe, segment, size, pleural effusion, additional metastasis, and their maximum standardized uptake value (SUV<sub>max</sub>) values were recorded, and survival analyses were performed.

**Results:** CLM developed in 125 cases. Eighty-one individuals had contralateral metastases at diagnosis, and 44 developed CLM during follow-up. Distant metastases were present in 100 patients; there was no CLM in the control group. While there was no statistical difference between the two groups in terms of the SUV<sub>max</sub>, mean standardized uptake, and metabolic tumor volume values, the presence of satellite nodules and metastatic nodules in other lobes in the same lung were found to be significantly higher in the CLM group (p=0.007; p<0.001). Also, in the CLM group, ipsilateral nodules had significantly higher SUV values than the control group (3.47 g/mL in the CLM group vs 2.81 g/mL in the control group; p=0.046). Pleural metastasis and effusion were more common in the CLM group (p=0.003; p=0.036). The mean SUV values in pleural metastases and pleural effusions in the CLM group were statistically significantly higher (p=0.048 and p=0.037). In statistical analyses, satellite nodules increase the probability of CLM fourfold, while ipsilateral other lobe nodules in the same lung increase it by 5.527 times (p=0.012; R=0.2752 and p=0.005; R=0.3672). Additionally, the absence of necrosis in the initial tumor raises the probability of metastasis to the contralateral lung by 3.326 times during follow-up (p=0.015; R=0.2656).

**Conclusion:** The study emphasized the role of ipsilateral nodules, pleural effusion, and pleural metastasis in predicting CLM using <sup>18</sup>F-FDG PET/CT imaging.

**Keywords:** <sup>18</sup>F-FDG PET/CT, lung cancer, contralateral spread, contralateral lung metastasis, pleural spread

**Address for Correspondence:** Büşra Özdemir Günay, Giresun Training and Research Hospital, Clinic of Nuclear Medicine, Giresun, Türkiye

**E-mail:** busraozdemir39@gmail.com **ORCID ID:** orcid.org/0000-0001-8540-0115

**Received:** 17.02.2025 **Accepted:** 24.08.2025 **Publication Date:** 08.10.2025

**Cite this article as:** Özdemir Günay B, Üstün F. <sup>18</sup>F-FDG PET/CT parameters and standard uptake values predicting contralateral lung metastasis in lung cancer. Mol Imaging Radionucl Ther. 2025;34:202-212.



Copyright© 2025 The Author. Published by Galenos Publishing House on behalf of the Turkish Society of Nuclear Medicine. This is an open access article under the Creative Commons Attribution-NonCommercial-NoDerivatives 4.0 (CC BY-NC-ND) International License.

## Öz

**Amaç:** Akciğer kanserinde kontralateral akciğer parankim metastazı (CLM), beklenenden daha az görülmekte olup kesin mekanizması hala bilinmemektedir. Bu çalışmada, akciğer kanserinde CLM'nin belirlenmesinde  $^{18}\text{F}$ -fluorodeoksiglukoz pozitron emisyon tomografisi/bilgisayarlı tomografinin ( $^{18}\text{F}$ -FDG PET/BT) ek değerini, nedenlerini ve prediktif faktörlerini ortaya koymak amaçlandı.

**Yöntem:** Veriler, CLM görülen grup ile CLM olmayan ancak diğer organlara uzak metastazı bulunan grup karşılaştırılarak değerlendirildi. Bu iki grup, akciğer kanserinde 9. tümör-nod-metastaz sınıflamasına göre M1 sınıflaması olarak tanımlanmaktadır. Histopatolojik veriler, takip bulguları ve primer tümör lobu, segmenti, boyutu, plevral efüzyon, ek metastazlar ile maksimum standardize tutulum değeri ( $\text{SUV}_{\text{max}}$ ) dahil olmak üzere  $^{18}\text{F}$ -FDG PET/BT bulguları kaydedildi ve sağkalım analizleri yapıldı.

**Bulgular:** Toplam 125 olguda CLM gelişti. Seksen bir hastada tanı sırasında kontralateral metastaz saptandı, 44 hastada ise takip sırasında CLM gelişti. Kontrol grubunda ise 100 hastada uzak metastaz varken CLM saptanmadı. İki grup arasında  $\text{SUV}_{\text{max}}$  ortalama standardize tutulum ve metabolik tümör hacmi değerleri açısından istatistiksel fark bulunmazken, aynı akciğerdeki diğer loblarda bulunan satellit nodüller ve metastatik nodüller CLM grubunda anlamlı derecede daha fazlaydı ( $p=0,007$ ;  $p<0,001$ ). Ayrıca CLM grubunda ipsilateral nodüllerin  $\text{SUV}$  değerleri, kontrol grubuna göre anlamlı derecede yüksekti (CLM grubunda  $3,47 \text{ g/mL}$ ; kontrol grubunda  $2,81 \text{ g/mL}$ ;  $p=0,046$ ). Plevral metastaz ve plevral efüzyon CLM grubunda daha sık görüldü ( $p=0,003$ ;  $p=0,036$ ). CLM grubunda plevral metastaz ve plevral efüzyonların ortalama  $\text{SUV}$  değerleri de istatistiksel olarak anlamlı derecede daha yüksekti ( $p=0,048$  ve  $p=0,037$ ). İstatistiksel analizlerde, satellit nodüller CLM olasılığını 4 kat artırırken, aynı akciğerin diğer lobundaki ipsilateral nodüller bu olasılığı 5,527 kat artırdı ( $p=0,012$ ;  $R=0,2752$  ve  $p=0,005$ ;  $R=0,3672$ ). Ayrıca, başlangıç tümöründe nekroz bulunmaması, takip sürecinde kontralateral akciğere metastaz gelişme olasılığını 3,326 kat artırdı ( $p=0,015$ ;  $R=0,2656$ ).

**Sonuç:** Çalışma,  $^{18}\text{F}$ -FDG PET/BT görüntüleme kullanılarak CLM öngörülmesinde ipsilateral nodüllerin, plevral efüzyonun ve plevral metastazın önemini vurgulamaktadır.

**Anahtar kelimeler:**  $^{18}\text{F}$ -FDG PET/BT, akciğer kanseri, kontralateral yayılım, kontralateral akciğer metastazı, plevral yayılım

## Introduction

Lung cancer is the second most frequent type of cancer worldwide, behind breast cancer in terms of incidence (1). The majority of lung cancer patients are diagnosed with metastatic disease, which considerably affects their prognosis. The 5-year survival rate for lung cancer is roughly 20%, indicating the percentage of patients who live at least five years after diagnosis (2). This low survival rate highlights the critical need for early detection and more effective treatments, as advanced-stage disease is much harder to treat successfully. The tumor-node-metastasis (TNM) staging system is the most-used approach for staging and directing treatment choices in primary lung cancer (3). Several studies have demonstrated the advantages of  $^{18}\text{F}$ -fluorodeoxyglucose positron emission tomography/computed tomography ( $^{18}\text{F}$ -FDG PET/CT) over standard conventional imaging methods in lung cancer, and the guidelines of the National Comprehensive Cancer Network recommend  $^{18}\text{F}$ -FDG PET/CT imaging for the evaluation of patients in all stages of lung cancer (4,5). The presence of a metastatic nodule and its location affect the patient's stage, while metastasis to the opposite lung, pericardium, or pleura is considered a distant metastatic disease (6). According to the 9<sup>th</sup> edition of the TNM classification, the M1a category includes patients with specific characteristics such as malignant pleural or pericardial effusion, and contralateral lung metastasis (CLM). Survival rates decrease significantly in cases of CLM; however, it is still better compared to patients with distant metastases to other

organs (3,7). Early detection and precise characterization of the metastatic pathways of CLM can result in improved survival rates. Early detection allows for prompt intervention, which may halt or reduce the progression of metastatic disease. Furthermore, identifying the exact metastatic pathways in CLM enables the development of targeted therapies and personalized treatment regimens.

In cases of lung cancer, CLM may not exhibit distinct clinical or radiological signs, as typically observed in metastases to other organs. Nonetheless, evidence suggests that surgical resection of contralateral metastatic lesions could contribute to improved overall survival outcomes. CLM poses significant challenges in determining optimal treatment protocols due to its association with poor prognosis. Consequently, early detection of CLM through accurate imaging is crucial for guiding treatment decisions. While conventional imaging modalities such as CT and magnetic resonance imaging have demonstrated limited sensitivity and specificity in identifying CLM,  $^{18}\text{F}$ -FDG PET/CT has shown superior diagnostic capability (3,4,5).  $^{18}\text{F}$ -FDG PET/CT not only enhances the detection of metastatic lesions but also provides critical insights into tumor grading and metastatic potential, making it a valuable tool in the clinical management of lung cancer (4,5).

The aim of this study is to determine the critical  $^{18}\text{F}$ -FDG PET/CT characteristics that, in the preoperative phase of lung cancer patients, can predict CLM. In cases where there are organ metastases outside the lung parenchyma, these parameters would be methodically compared with

surgical and histological findings. The best cut-off levels will be determined by examining standard uptake value maximum ( $SUV_{max}$ ) values in order to improve diagnostic precision. By evaluating  $^{18}F$ -FDG PET/CT's effectiveness as a non-invasive diagnostic tool, the evaluation seeks to enhance clinical judgment in the treatment of lung cancer.

## Materials and Methods

### Patients

Retrospective analysis was performed on 225 cases between October 2015 and December 2021. Of these, 125 had been diagnosed with lung cancer and had CLM in  $^{18}F$ -FDG PET/CT imaging at diagnosis and during follow-up (CLM group), and 100 had distant metastases, CLM during the follow-up (control group).

Gender, age at the time of diagnosis, postoperative histopathological data,  $^{18}F$ -FDG PET/CT findings including primary tumor lobe, segment, size, tumor contours, necrosis, pleural effusion, pleural involvement, mediastinal invasion, thorax wall invasion, ipsilateral lung metastasis, and additional metastasis were recorded. Patients TNM stages were recorded based on  $^{18}F$ -FDG PET/CT.

We compared data from 44 patients who developed CLM in follow up, and 100 patients who had distant metastases (control group) to determine which factors predict contralateral metastasis. In addition, imaging and  $^{18}F$ -FDG PET/CT findings that could predict the possibility of metastasis were analyzed in groups with and without CLM.

This study was performed in accordance with the ethical concepts of the October 2013 Helsinki Declaration and approved by the institutional ethical review board Ethics Committee of Scientific Research, Dean's Office, Faculty of Medicine, Trakya University (number: TUTF BAEK-2020/299, date: 24.08.2020).

### Imaging and Image Analysis

All patients fasted for at least 4 hours until reaching a blood sugar level lower than 170 mg/dL before the injection of  $^{18}F$ -FDG, and oral contrast was administered. Approximately 3.7 MBq/kg of  $^{18}F$ -FDG was injected intravenously into the patients. After one hour,  $^{18}F$ -FDG PET/CT scans were performed from the skull to the mid-thigh, 3 min per bed position, and with iterative reconstruction using a combined PET/CT system (Discovery STE; GE Medical Systems, Milwaukee, WI).  $^{18}F$ -FDG PET/CT fusion images were created, and axial, coronal, and sagittal images were reformatted.

$^{18}F$ -FDG PET/CT images were interpreted in PET VCAR software (GE Healthcare) by a nuclear medicine physician without any information about the patient.

$^{18}F$ -FDG PET/CT images showing greater FDG uptake than normal organs or surrounding tissues were classified as metastatic lesions. In the case of lung nodules, the CT component was evaluated and any suspicious opacity was determined as a possible lung metastasis. By reviewing follow-up  $^{18}F$ -FDG PET/CT, CT, and magnetic resonance images, as well as histological analysis and treatment response, a consensus was reached on the classification of lesions as metastatic.

The  $SUV_{max}$  mean standardized uptake ( $SUV_{mean}$ ), and metabolic tumor volume (MTV) values were calculated for primary tumors and metastatic lesions. Regions of interest of the lesions were reviewed using a threshold of 42% of the tumor  $SUV_{max}$  or greater.

### Statistical Analysis

Statistical analyses were conducted using SPSS version 25 (SPSS, Inc., Chicago, IL). Student's t-tests were used to analyze paired samples. Categorical variables were compared using the  $\chi^2$  and Fisher's exact tests. Pearson's r correlation coefficient and Spearman's rank correlation coefficient were used to analyze the relationship between continuous variables. One-way ANOVA or Kruskal-Wallis tests were used to compare groups, followed by Tukey post-hoc tests for continuous variables. All p values less than 0.05 were considered statistically significant. Kaplan-Meier estimations were used to create survival curves.

## Results

### Patient and Tumor Characteristics

The study included 225 patients undergoing  $^{18}F$ -FDG PET/CT (30 females, 195 males). The mean age at the time of diagnosis was  $61.8 \pm 9.2$  (38-85) years in the contralateral lung parenchyma group (CLM group) and  $61.4 \pm 8.2$  (30-78) years in the control group. Histopathological diagnoses were 57 adenocarcinomas, 50 squamous cell carcinomas, 6 large cell carcinomas, and 12 small cell carcinomas in the CLM group. 47 adenocarcinomas, 30 squamous carcinomas, 4 large cell carcinomas, and 19 small cell carcinomas were observed in the control group, respectively. There was no association found between tumor histology and CLM ( $p=0.156$ ). Table 1 provides details of patient and tumor characteristics. When patients were staged based on  $^{18}F$ -FDG PET/CT findings, 43 patients had M1a, 16 had M1b, and 66 of them had M1c disease in the CLM group.

In a subgroup of 44 patients, who developed CLM during follow-up, the mean age in this group was  $62.4 \pm 10.2$  (38-83). Nineteen adenocarcinomas, 23 squamous cell carcinomas, 1 large cell carcinoma, and 1 small cell

carcinoma were observed in CLM in the follow-up group. There was no significant variance between the histological categories in terms of the development of CLM during follow-up ( $p=0.231$ ).

Primary tumors' locations are defined as lobes and segments based on the CT component of  $^{18}\text{F}$ -FDG PET/CT. Primary tumors could not be evaluated due to prior surgery in 7 patients in the CLM group and 8 patients in the control group. When the location of the primary lung tumor and metastasis to the contralateral lung parenchyma were assessed, there was no statistically significant correlation between tumor localization and metastasis ( $p=0.314$ ). In addition, when we differentiated primary tumors that originated from either the lower lobe or the upper lobe, no significant difference was found in terms of the risk of metastasis to the opposite lung parenchyma (0.176). Throughout the follow-up, there was no significant correlation between tumor localization and the development of opposite parenchymal metastases ( $p=0.320$  and  $p=0.241$ ).

#### $^{18}\text{F}$ -FDG PET/CT Findings

The metabolic parameters of primary tumors of the 225 patients were evaluated. The mean  $\text{SUV}_{\text{max}}$ ,  $\text{SUV}_{\text{mean}}$ , and MTV of the primary tumors were 14.9 g/mL, 8.8 g/mL, and 52.75  $\text{cm}^3$ , respectively.  $\text{SUV}_{\text{max}}$ ,  $\text{SUV}_{\text{mean}}$ , and MTV of the main tumor on  $^{18}\text{F}$ -FDG PET/CT did not differ significantly between the CLM group and the group that developed metastasis during follow-up compared to the control groups ( $p=0.187$ ;  $p=0.167$ ;  $p=0.873$  in CLM group and  $p=0.274$ ;  $p=0.212$ ;  $p=0.104$  in the CLM in follow-up group).

In the CLM group, there were 24 patients with mediastinal invasion and 7 patients with thoracic wall invasion, compared to 19 patients with mediastinal invasion and 4 patients with thoracic wall invasion in the control group

( $p=0.545$  and  $p=0.426$ ). Thirty-one patients in the control group, and 44 patients in the CLM group had necrotic components in their primary tumors ( $p=0.347$ ).

Metastatic nodules are categorized based on  $^{18}\text{F}$ -FDG PET/CT as one nodule, oligo-metastatic nodules, and multiple nodules. Thirty-three patients had a single nodule in the contralateral lung, 63 patients had oligo-metastatic nodules, and 29 patients had multiple contralateral nodules in  $^{18}\text{F}$ -FDG PET/CT. Mean dimensions of the contralateral nodules was  $14.6 \pm 6.9$  mm (2.3 to 29 mm) and mean  $\text{SUV}_{\text{max}}$  of the contralateral nodules was  $4.6 \pm 4.4$  (min 0.4 and max 29.9 g/mL).

In the CLM group, 65 (52%) patients had satellite nodules that were metastatic nodules in the same lobe as the primary. Additionally, 65 (52%) patients had metastatic nodules in the ipsilateral other lobe, with a mean dimension of  $12.2 \pm 4.3$  mm and a mean  $\text{SUV}_{\text{max}}$  of 3.47 g/mL. In the control group, 34 (34%) patients had satellite nodules and 20 (20%) patients had nodules in the ipsilateral lobe with a mean dimension of  $13.9 \pm 3.4$  mm, a mean  $\text{SUV}_{\text{max}}$  of 2.81 g/mL. A satellite nodule and an ipsilateral nodule were observed to be significantly more common in the CLM group than in the control group ( $p=0.007$  and  $p<0.001$ , respectively). There was no difference in the mean dimension of ipsilateral nodules between the two groups ( $p=0.432$ ), but in the CLM group, ipsilateral nodules had significantly higher SUV values than the control group ( $p=0.046$ ).

Figure 1 shows a patient who had both an ipsilateral satellite nodule and a metastatic nodule in the contralateral lung at the time of diagnosis.  $\text{SUV}_{\text{max}}$  of the patient's primary lesion was 9.7 g/mL, ipsilateral nodules  $\text{SUV}_{\text{max}}$  was 5.2 g/mL, and contralateral nodules  $\text{SUV}_{\text{max}}$  was 3.1 g/mL.

Among the concomitant findings, pleural metastases were found in 55 patients in the CLM group and in 25 patients

**Table 1. Patients and tumor characteristics**

|                         | CLM group (n: 125) | Control group (n: 100) |
|-------------------------|--------------------|------------------------|
| <b>Gender</b>           |                    |                        |
| Male                    | 106                | 89                     |
| Female                  | 19                 | 11                     |
| <b>Age</b>              | $61.8 \pm 9.2$     | $61.4 \pm 8.2$         |
| <b>Pathology</b>        |                    |                        |
| Adenocarcinoma          | 57                 | 47                     |
| Squamous cell carcinoma | 50                 | 30                     |
| Large cell carcinoma    | 6                  | 4                      |
| Small cell carcinoma    | 12                 | 19                     |

CLM: Contralateral lung parenchymal metastasis

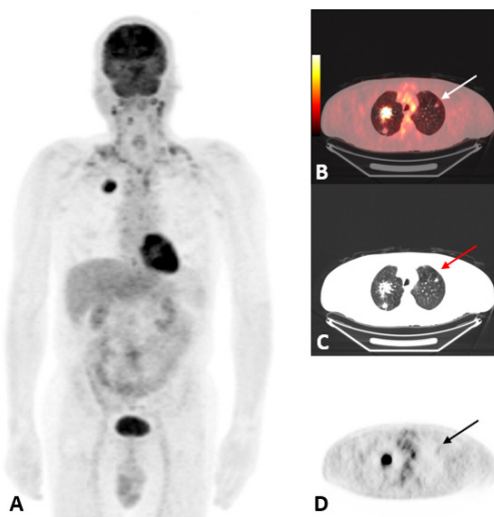


**Figure 1.** (A-D) A patient who had both an ipsilateral satellite nodule and a metastatic nodule in the contralateral lung at the MIP image (A) and and this patient's contralateral lung metastasis (arrows) (B-D) at the time of diagnosis.  $SUV_{max}$  of the primary lesion was 9.7 g/mL

$SUV_{max}$ : Standardized uptake value, MIP: Maximum intensity projection

in the control group ( $p=0.003$ ). Pleural effusion was found in 42 patients in the CLM group and in 21 patients in the control group ( $p=0.025$ ). The findings are summarized in Table 2. The mean SUV values in pleural metastases in the CLM group were 5.42 g/mL, and a statistically significant difference was found in the mean SUV values in the non-CLM group, with 4.17 g/mL ( $p=0.048$ ). Similarly, the mean SUV value in the CLM group with pleural effusion was 3.25 g/mL while the SUV value in the non-CLM group with pleural effusion was 2.11g/mL. A statistically significant difference was found ( $p=0.037$ ).

When the patients were grouped according to the stages of the mediastinal lymph nodes, there were 7 patients in the N1 stage, 27 patients in the N2 stage and 54 patients in the N3 stage in the CLM group, while there were 5 patients in the N1 stage, 25 patients in the N2 stage and 47 patients in the N3 stage in the control group. Mediastinal lymph node positivity and stage were not significantly correlated with CLM ( $p=0.547$ ).

A total of 41 (32.8%) patients showed PET-positive bone metastases, with an average  $SUV_{max}$  of  $11.8 \pm 6.4$ . Thirty-one (24.8%) patients had PET-positive adrenal metastasis, with an average  $SUV_{max}$  of  $7 \pm 4.8$ . A total of 18 patients (14.4%) showed PET-positive liver metastases, with an average

**Table 2. Characteristics of primary tumor, ipsilateral metastatic nodules and pleural involvement between two group and their p values**

|                                    | CLM group | Control group | p       |
|------------------------------------|-----------|---------------|---------|
| <b>Mediastinal invasion</b>        |           |               | NS      |
| Negative                           | 94        | 73            |         |
| Positive                           | 24        | 19            |         |
| <b>Thoracic wall invasion</b>      |           |               | NS      |
| Negative                           | 111       | 88            |         |
| Positive                           | 7         | 4             |         |
| <b>Necrosis</b>                    |           |               | NS      |
| Negative                           | 74        | 61            |         |
| Positive                           | 44        | 31            |         |
| <b>Pleural metastasis</b>          |           |               | 0.003*  |
| Negative                           | 70        | 75            |         |
| Positive                           | 55        | 25            |         |
| <b>Pleural effusion</b>            |           |               | 0.025*  |
| Negative                           | 83        | 79            |         |
| Positive                           | 42        | 21            |         |
| <b>Ipsilateral lung metastasis</b> |           |               |         |
| Same lobe                          | 65        | 34            | 0.007*  |
| Other lobe                         | 65        | 30            | <0.001* |

\*: statistically significant, CLM: Contralateral lung parenchymal metastasis, NS: Not significant



SUV<sub>max</sub> of 11.5±6. Thirteen patients (10.4%) had brain metastases, and six (4.8%) had soft tissue metastases.

When distant node metastasis was evaluated, twenty-six (20.8%) had neck lymph node metastasis and twenty-two (17.6%) had abdominal lymph node metastasis, with an average SUV<sub>max</sub> of 6.7±4.6. All these findings did not significantly correlate with the CLM.

When the characteristics of the group that developed CLM during follow-up were compared to the control group, no significant difference was found between histopathological subtypes in terms of developing CLM during follow-up ( $r=0.1321$ ,  $p=0.231$ ).

Similar to the CLM group, no significant difference was detected in terms of SUV<sub>max</sub>, SUV<sub>mean</sub>, and MTV values of the primary lesions between CLM in the follow-up group and the control group ( $p=0.274$ ;  $p=0.212$  and  $p=0.104$ ).

Among the evaluated parameters: mediastinal lymph node metastasis stage ( $p=0.547$ ), supraclavicular lymph node metastasis ( $p=0.422$ ) and metastasis to the other neck lymph nodes ( $p=0.877$ ), and presence of abdominal lymph node metastasis ( $p=0.381$ ) did not contribute significantly to predicting contralateral lung parenchymal metastasis during follow-up. Also, the presence of distant metastases such as bone ( $p=0.858$ ), liver ( $p=0.291$ ), adrenal ( $p=0.264$ ),

soft tissue ( $p=0.064$ ), brain metastases ( $p=0.614$ ) and their SUV values did not contribute significantly to predicting CLM during follow up.

The factors predicting the development of CLM in the follow-up were as follows;

1- Satellite nodules in the same lobe raise the probability of CLM by fourfold [ $p=0.012$ ;  $R=0.2752$ ; 95% confidence interval (CI): 0.082-0.767].

2- Nodules in the other ipsilateral lobe raise the probability of CLM by 5.527 times ( $p=0.005$ ;  $R=0.3672$ ; 95% CI: 0.042-0.563).

3- The absence of necrotic features in the initial tumor increases the likelihood of metastasis to the contralateral lung parenchyma by 3.326 times ( $p=0.015$ ;  $R=0.2656$ ; 95% CI: 1.236-8.950).

There was no significant difference between the two groups when the other associated findings were compared. The findings are summarized in Table 3.

### Overall Survival

Median follow up time was 19.9 months (minimum: 1, maximum: 123). In the follow-up, 110 (88%) patients died in the CLM group and 94 (94%) patients died in the control group.

**Table 3. Characteristics of primary tumor, ipsilateral metastatic nodules, pleural involvement and their p values between CLM in follow up and control group**

|                                    | CLM in follow up group | Control group | p      |
|------------------------------------|------------------------|---------------|--------|
| <b>Mediastinal invasion</b>        |                        |               |        |
| Negative                           | 40                     | 73            | NS     |
| Positive                           | 4                      | 19            |        |
| <b>Thoracic wall invasion</b>      |                        |               |        |
| Negative                           | 44                     | 88            | NS     |
| Positive                           | 0                      | 4             |        |
| <b>Necrosis</b>                    |                        |               | 0.015* |
| Negative                           | 36                     | 61            |        |
| Positive                           | 8                      | 31            |        |
| <b>Pleural metastasis</b>          |                        |               | NS     |
| Negative                           | 37                     | 75            |        |
| Positive                           | 7                      | 25            |        |
| <b>Pleural effusion</b>            |                        |               | NS     |
| Negative                           | 36                     | 79            |        |
| Positive                           | 8                      | 21            |        |
| <b>Ipsilateral lung metastasis</b> |                        |               |        |
| Same lobe                          | 16                     | 34            | 0.012* |
| Other lobe                         | 10                     | 30            | 0.005* |

\*: statistically significant, CLM: Contralateral lung parenchymal metastasis, NS: Not significant

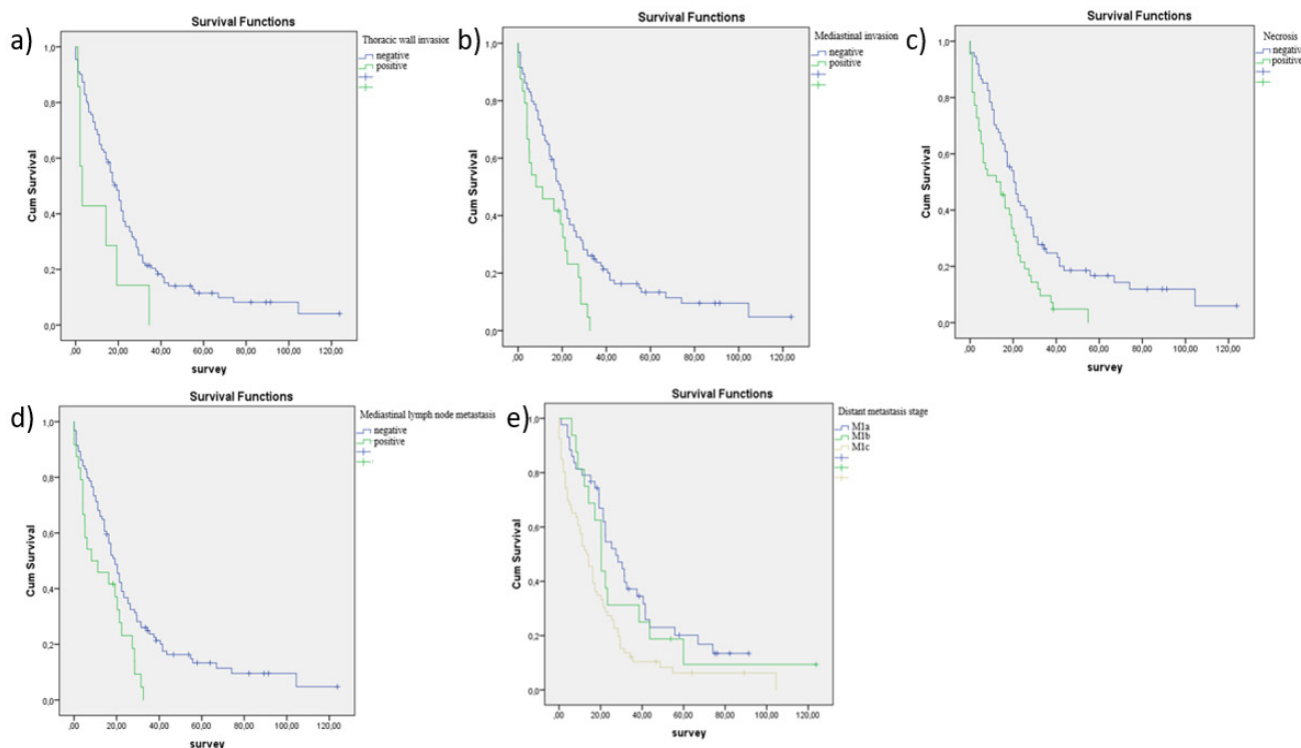


**Figure 2.** (A-E) Survival curves shown based on the significant predictors

When divided based on distant metastases, in the CLM group, 43 patients were at the M1a stage, 16 patients were at the M1b stage, and 66 patients were at the M1c stage. In the control group, 22 patients were found in the M1b stage and 78 patients were found in the M1c stage.

The median duration of life was 35.7 months in the M1a group, which had only CLM. In the M1b group, which had distant metastases to a single organ, median lifetime was 33.2 months, and in the M1c group, which had multiple distant metastases, the median lifetime was 20.1 months. The M1b and M1a groups did not show any significant differences in survival ( $p=0.497$ ); however, there was a significant difference in survival between the M1a and M1c groups ( $p=0.001$ ).

When analyzed separately, the overall 1-year survival rate was 0.65 and 5-year survival rate was 0.08 in the CLM group. The 1-year survival rate was 0.44 and the 5-year survival rate was 0.02 in the control group, respectively. In terms of overall survival, there was a substantial difference between the CLM group and the control group ( $p<0.001$ ). The average survival of patients with CLM was 28.3 months, and the control group was 15.5 months.

In the CLM group, only small cell lung cancer showed a significantly shorter survival time compared to adenocarcinoma and squamous cell carcinoma ( $p=0.001$ ). There was no association in survival for other subtypes.

The factors significantly correlated with patient survival include thoracic wall invasion ( $p=0.044$ , a), mediastinal invasion ( $p=0.008$ , b), presence of necrosis in primary tumor ( $p=0.001$ , c), mediastinal lymph node involvement ( $p=0.030$ , d), and stage of distant metastasis ( $p=0.002$ , e). In Figure 2, survival curves are shown based on the significant predictors.

When we analyzed the association between contralateral nodule features and survival, there was no significant difference in surveillance regarding the number, size, or  $SUV_{max}$  of contralateral parenchymal metastases ( $p=0.698$ ;  $p=0.447$ ;  $p=0.352$ ).

## Discussion

This study aims to identify  $^{18}F$ -FDG PET/CT features that predict CLM in lung cancer patients. For several years, researchers have extensively investigated the phenomenon of CLM lung cancer, proposing various hypotheses

regarding its mechanisms of dissemination. Notably, Ferguson et al. (8) reported that CLM occurs infrequently, even in cases where there is mediastinal involvement. This finding suggests that the pathways of metastatic spread to the contralateral lung may differ from those to other organs, underscoring the need for further research to elucidate the specific biological and pathological processes governing CLM. By accurately diagnosing the tumor grade and contralateral development,  $^{18}\text{F}$ -FDG PET/CT helps improve the clinical care for patients.

Onuigbo (9) examined the spread of lung cancer and the mechanisms underlying CLM. The article highlights several key factors: anatomically, both lungs share a similar microenvironment; the contralateral lung is one of the closest organs to the primary tumor; and the lungs receive their blood supply directly from the aorta. Additionally, both lungs are interconnected through venous and lymphatic collaterals. Despite these considerations, Onuigbo (9) proposed a novel explanation for the relatively infrequent occurrence of metastasis to the contralateral lung: although cancer cells do reach the opposing lung, they disappear before they can adhere and establish a metastatic focus.

In our study, satellite nodules in the same lobe with the primary and metastatic nodules in the ipsilateral other lobe were frequently observed in CLM, suggesting that not only tumor grade or burden but also specific routes might affect metastasis to the contralateral lung. The mechanism by which the contralateral lung is spread to could be the reason for the frequent occurrence of CLM. This finding may be consistent with the view stated in Onuigbo's study (9), that although cancer cells reach the opposite lung, they disappear without being able to establish there. In addition, studies on lymphatic drainage have shown that the visceral lymphatic circulation connects the two lungs (10). In the study we performed,  $\text{SUV}_{\text{max}}$  values for satellite nodules or nodules in the same lobe that developed CLM were 3.47 g/mL. Quantifying  $\text{SUV}_{\text{max}}$  values of ipsilateral nodules in  $^{18}\text{F}$ -FDG PET/CT scans may help predict CLM by identifying high tumor burden that could metastasize between lungs. This measurement is crucial because it enables us to better identify the tumor's biological behavior and spread potential. Specifically, elevated FDG uptake identified using  $^{18}\text{F}$ -FDG PET/CT indicates a more aggressive biological behavior of the tumor or a greater number of tumor cells disseminated through the lung lymphatics, raising the likelihood of metastasis to the opposing lung. Because of the useful information  $^{18}\text{F}$ -FDG PET/CT offers in the assessment of metastatic spread, it is an essential tool in the clinical decision-making process and plays a significant role in directing patient care.

Patients with lung cancer who have pleural effusion frequently have advanced disease and a bad prognosis (11). According to a study, 20% of cases of lung cancer and pleural effusion are discovered at the time of diagnosis (12). In our study, 28% of patients with lung cancer had pleural effusions, and 66.6% of these individuals had CLM. A meta-analysis by Treglia et al. (13) demonstrated that  $^{18}\text{F}$ -FDG PET/CT has 86% sensitivity and 80% specificity in detecting pleural abnormalities.

The diagnostic accuracy of malignant and benign pleural effusions was evaluated by  $^{18}\text{F}$ -FDG PET/CT imaging, more specifically by calculating  $\text{SUV}_{\text{max}}$ . In the study by Simsek et al. (14), the specificity and positive predictive value for  $\text{SUV}_{\text{max}} > 1.3$  were found to be 100%, although the sensitivity was suboptimal. Furthermore, Nakajima et al. (15) emphasize that cytological evaluations cannot provide a definitive diagnosis in up to 30% of cases, and that imaging methods, especially  $^{18}\text{F}$ -FDG PET/CT, should be relied upon for more accurate differentiation. In our investigation, the  $\text{SUV}_{\text{max}}$  values of pleural effusions associated with CLM were assessed as 3.25 g/mL, whereas the  $\text{SUV}_{\text{max}}$  values of pleural effusions unassociated with CLM were measured as 2.11 g/mL, indicating a clinically significant difference. Furthermore, our findings contribute to the current literature by revealing that greater SUV values of a pleural effusion are related to an increased likelihood of malignant pleural effusion and a higher risk of developing CLM. These findings make an important contribution to conventional imaging and cytological sampling procedures.

This emphasizes how crucial it is to incorporate metabolic data into the therapeutic setting in order to improve the precision of diagnosis. Because  $^{18}\text{F}$ -FDG PET/CT can objectively detect metabolic activity by SUV values, it offers a non-invasive method of evaluating tumor aggressiveness and survival.

Pleural involvement in lung cancer has been recognized as a substantial risk factor for CLM. It promotes tumor cell spread through the lymphatic system and pleural space, increasing the risk of metastasis to the opposite lung. Lymphatic routes may allow tumor cells on the pleural surface to spread to the contralateral lung and diaphragm. According to studies metastasis usually starts with ipsilateral pleural involvement, then spreads to the contralateral pleura, and finally invades the contralateral lung parenchyma, without any blood vessel involvement (9,10,16,17).

In Rashidi et al.'s (18) experimental study, lung cancer cells have been reported to migrate to the diaphragmatic surface via lymphatic pathways in the ipsilateral lung. Most of the cells reached the contralateral diaphragmatic



surface, and only a small percentage proceeded through the bronchovascular pedicle to reach the contralateral lung parenchyma.

Several studies have shown that the presence of pleural effusion and pleural metastases increases the incidence of metastatic lesions in the contralateral lung parenchyma (19,20,21,22). In our study, we found that the incidence of metastasis in the contralateral lung parenchyma was higher in cases with ipsilateral pleural involvement consistent with the literature. According to these data, pleural involvement in lung cancer patients can be regarded as a significant indicator that worsens the prognosis of the illness and raises the possibility of metastatic dissemination. Evidence suggests that pleural effusion and pleural metastases have been associated with an increased risk of metastatic lesions in the contralateral lung parenchyma. However, the intensity of this link differs between studies, emphasizing the need for further research to understand the underlying mechanisms and therapeutic implications.

The relationship between necrotic tissue and lung cancer involves various biological mechanisms that affect tumor behavior and treatment outcomes (23). Necrosis in tumor cells could influence the tumor microenvironment, immune response, and treatment efficacy, although its effect on prognosis and therapy results in lung cancer is unknown (24). Future research should look into how necrosis influences drug delivery, immune cell infiltration, and inflammation, potentially affecting therapeutic responses. Our study indicated that the risk of metastasis to the contralateral lung parenchyma increased 3.326 times during the follow-up period in tumors without necrosis compared to primary necrotic lung masses. This suggests that tumors with less necrosis may have a more robust vascular network, which may facilitate the continued growth of the tumor and the spread of malignant cells to distant sites. The lack of necrosis within the primary tumor may indicate that the tumor is in a well-vascularized environment, which supports its sustainable growth and metastasis potential. In this context, the low amount of necrotic tissue and the high presence of viable tissue may play a more important role tumor grade and prognosis, and may determine the course of the disease and response to treatment. Onuigbo (17) explained in their study on lung cancer that the lower incidence of metastasis to the opposite lung parenchyma could be attributed to significant necrosis development in tumor cells that reach the pleura of the opposite lung through the lymphatic route. This could be because these tumors were sensitive to factors secreted during necrosis. As a result, the primary tumor's sensitivity to these factors

may lead to the elimination of metastatic cells by the contralateral lung before they can establish lesions during their invasion of the other lung.

Apart from conventional imaging findings,  $^{18}\text{F}$ -FDG PET/CT provides information about tumor biology and tumor heterogeneity, by showing necrotic tissue. Although there are no specific data on tumor heterogeneity in our study, the effect of the presence of necrosis on CLM has been clearly demonstrated. Tumor heterogeneity may have an important role in predicting CLM, and future studies on this subject are needed. Besides high  $\text{SUV}_{\text{max}}$  values in tumors, necrotic areas may be associated with an increased risk of metastasis, and this finding is of great importance in evaluation both metabolic imaging and CLM.

Previous studies primarily aimed to determine whether a nodule detected in the contralateral lung is malignant. Two of these studies found that malignant contralateral nodules are typically adenocarcinomas (25,26). In contrast, Carretta et al. (27) observed no significant association between the initial tumor histology and the presence of metastatic nodules in the lung. Similarly, our study suggests that histopathological subtypes did not affect CLM or the development of metastasis during follow-up.

The lobe or segment location of original tumors did not correlate with the location where CLM were more frequently identified in our investigation. On the other hand, Huang et al. (28) showed that initial tumors in the upper lobe were associated with metastases in the upper lobe of the contralateral lung in patients with adenocarcinoma. Larger prospective studies are required to validate these results, and elucidate the significance of various subtypes, especially those that concentrate on pure histopathological subtypes.

Sánchez de Cos Escuín et al. (29) demonstrated in a previous study that the number of CLM, whether single or multiple, has no effect on survival. In a study by Rami-Porta and Eberhardt (16) that examined the IASLC database, the researchers hypothesized that the presence of multiple metastatic nodules may have a worse prognosis than the presence of a single nodule, but it did not create a statistically significant result due to the low number of patients. In our study, no significant correlation was found between the number of CLM and survival. There was no association between survival and the size or  $\text{SUV}_{\text{max}}$  values of metastatic nodules in the contralateral lung. To the best of our knowledge, this is the first study to assess the association between the number of contralateral metastatic lung nodules as well as their  $\text{SUV}_{\text{max}}$  values with survival.

### Study Limitations

As a limitation of the study, because it was conducted retrospectively, we included patients with proven contralateral metastases, resulting in selection bias. Not all lesions could be correlated histopathologically as metastatic in the contralateral lung. However, additional imaging and clinical follow-ups aid in the characterization of the lesions. Since the treatments received by the patients were not evaluated in this study, data related to treatment could not be presented in the survival analyses. Nevertheless, the strengths of the study include the interpretation of all  $^{18}\text{F}$ -FDG PET/CT, imaging, and all pathologies, at our university hospital. Further prospective studies are needed to confirm our findings and identify predictive factors.

### Conclusion

In conclusion, the study indicated the importance of ipsilateral nodules, pleural effusion, and pleural metastasis in utilizing  $^{18}\text{F}$ -FDG PET/CT imaging to predict CLM. These results demonstrate the significance of  $^{18}\text{F}$ -FDG PET/CT as a useful diagnostic tool for locating and evaluating lung cancer patients' metastatic pathways, which helps with more precise prediction of outcomes and treatment planning. In the management of lung cancer, more investigation and validation of these prognostic indicators may improve clinical expertise and patient outcomes.

### Acknowledgment

The authors thank MD, Prof. Necdet Süt for his contribution to the statistical analyses. Also, I would like to thank my husband MD, Burak Günay for his support and always being there for me.

### Ethics

**Ethics Committee Approval:** This study was performed in accordance with the ethical concepts of the October 2013 Helsinki Declaration and approved by the institutional ethical review board Ethics Committee of Scientific Research, Dean's Office, Faculty of Medicine, Trakya University (number: TUTF BAEK- 2020/299, date: 24.08.2020).

**Informed Consent:** Retrospective study.

### Footnotes

#### Authorship Contributions

Surgical and Medical Practices: F.Ü., Concept: B.Ö.G., F.Ü., Design: F.Ü., Data Collection or Processing: B.Ö.G., Analysis or Interpretation: B.Ö.G., Literature Search: B.Ö.G., F.Ü., Writing: B.Ö.G., F.Ü.

**Conflict of Interest:** No conflict of interest was declared by the authors.

**Financial Disclosure:** The authors declared that this study has received no financial support.

### References

1. Sung H, Ferlay J, Siegel RL, Laversanne M, Soerjomataram I, Jemal A, Bray F. Global Cancer Statistics 2020: GLOBOCAN estimates of incidence and mortality worldwide for 36 cancers in 185 countries. *CA Cancer J Clin.* 2021;71:209-249.
2. Akdemir ÜÖ, Aydos U. Role of fluorodeoxyglucose positron emission tomography/computed tomography imaging in diagnosis and staging of lung cancer. *Nucl Med Semin.* 2018;4:6-17.
3. Kandathil A, Kay FU, Butt YM, Wachsmann JW, Subramaniam RM. Role of FDG PET/CT in the eighth edition of TNM staging of non-small cell lung cancer. *Radiographics.* 2018;38:2134-2149.
4. Deppen SA, Blume JD, Kensinger CD, Morgan AM, Aldrich MC, Massion PP, Walker RC, McPheeters ML, Putnam JB Jr, Grogan EL. Accuracy of FDG-PET to diagnose lung cancer in areas with infectious lung disease: a meta-analysis. *JAMA.* 2014;312:1227-1236.
5. Kubota K, Matsuno S, Morioka N, Adachi S, Koizumi M, Seto H, Kojo M, Nishioka S, Nishimura M, Yamamoto H. Impact of FDG-PET findings on decisions regarding patient management strategies: a multicenter trial in patients with lung cancer and other types of cancer. *Ann Nucl Med.* 2015;29:431-441.
6. Eberhardt WE, Mitchell A, Crowley J, Kondo H, Kim YT, Turrisi A 3rd, Goldstraw P, Rami-Porta R; International association for study of lung cancer staging and prognostic factors committee, advisory board members, and participating institutions. the IASLC lung cancer staging project: proposals for the revision of the m descriptors in the forthcoming eighth edition of the TNM classification of lung cancer. *J Thorac Oncol.* 2015;10:1515-1522.
7. Shin J, Keam B, Kim M, Park YS, Kim TM, Kim DW, Kim YW, Heo DS. Prognostic impact of newly proposed m descriptors in TNM classification of non-small cell lung cancer. *J Thorac Oncol.* 2017;12:520-528.
8. Ferguson MK, DeMeester TR, DesLauriers J, Little AG, Piraux M, Golomb H. Diagnosis and management of synchronous lung cancers. *J Thorac Cardiovasc Surg.* 1985;89:378-385.
9. Onuigbo WI. Anomalous lung cancer cell carriage: a historical review with present prospects. *Int J Surg.* 2014;12:734-746.
10. Riquet M. Bronchial arteries and lymphatics of the lung. *Thorac Surg Clin.* 2007;17:619-638.
11. Skok K, Hladnik G, Grm A, Crnjac A. Malignant pleural effusion and its current management: a review. *Medicina (Kaunas)* 2019;55:490.
12. Lombardi G, Zustovich F, Nicoletto MQ, Donach M, Artioli G, Pastorelli D. Diagnosis and treatment of malignant pleural effusion: a systematic literature review and new approaches. *Am J Clin Oncol.* 2010;33:420-423.
13. Treglia G, Sadeghi R, Annunziata S, Lococo F, Cafarotti S, Prior JO, Bertagna F, Ceriani L, Giovannella L. Diagnostic performance of fluorine-18-fluorodeoxyglucose positron emission tomography in the assessment of pleural abnormalities in cancer patients: a systematic review and a meta-analysis. *Lung Cancer.* 2014;83:1-7.
14. Simsek FS, Yuksel D, Yaylali O, Aslan HS, Kılıçarslan E, Bir F, Arslan M, Can FE, Ugurlu E. Can PET/CT be used more effectively in pleural effusion evaluation? *Jpn J Radiol.* 2021;39:1186-1194.
15. Nakajima R, Abe K, Sakai S. Diagnostic ability of FDG-PET/CT in the detection of malignant pleural effusion. *Medicine (Baltimore).* 2015;94:e1010.

16. Rami-Porta R, Eberhardt WEE. Clinical implications of the innovations in the primary tumour and metastasis of the 8<sup>th</sup> edition of the TNM classification for lung cancer. *J Thorac Dis.* 2018;10(Suppl 22):2682-2685.
17. Onuigbo WI. Contralateral pulmonary metastases in lung cancer. *Thorax.* 1974;29:132-133.
18. Rashidi B, Moossa AR, Hoffman RM. Specific route mapping visualized with GFP of single-file streaming contralateral and systemic metastasis of Lewis lung carcinoma cells beginning within hours of orthotopic implantation [correction of implantation]. *J Cell Biochem.* 2013;114:1738-1743.
19. Kruse M, Sherry SJ, Paidpally V, Mercier G, Subramaniam RM. FDG PET/CT in the management of primary pleural tumors and pleural metastases. *AJR Am J Roentgenol.* 2013;201:W215-W226.
20. Mordant P, Rivera C, Legras A, Le Pimpec Barthes F, Riquet M. Current readings: the most influential and recent studies regarding resection of lung cancer in m1a disease. *Semin Thorac Cardiovasc Surg.* 2013;25:251-255.
21. Zutić H. [Bronchial carcinoma—an overview]. *Med Arh.* 1999;53(3 Suppl 1):27-31.
22. Svaton M, Havel D, Buresova M, Baxa J, Hosek P. Percutaneous transthoracic needle biopsy of lung lesions is a safe method associated with a very low risk of pleural recurrence. *Biomed Pap Med Fac Univ Palacky Olomouc Czech Repub.* 2025;169:21-25.
23. Butter R, Halfwerk H, Radonic T, Lissenberg-Witte B, Thunnissen E. The impact of impaired tissue fixation in resected non-small-cell lung cancer on protein deterioration and DNA degradation. *Lung Cancer.* 2023;178:108-115.
24. Kludt C, Wang Y, Ahmad W, Bychkov A, Fukuoka J, Gaisa N, Kühnel M, Jonigk D, Pryalukhin A, Mairinger F, Klein F, Schultheis AM, Seper A, Hulla W, Brägelmann J, Michels S, Klein S, Quaas A, Büttner R, Tolbach Y. Next-generation lung cancer pathology: development and validation of diagnostic and prognostic algorithms. *Cell Rep Med.* 2024;5:101697.
25. Ruppert AM, Lerolle U, Carette MF, Lavole A, Khalil A, Bazelly B, Antoine M, Cadranet J, Milleron B. Coexisting pulmonary nodules in operable lung cancer: prevalence and probability of malignancy. *Lung Cancer.* 2011;74:233-238.
26. Riihimäki M, Hemminki A, Fallah M, Thomsen H, Sundquist K, Sundquist J, Hemminki K. Metastatic sites and survival in lung cancer. *Lung Cancer.* 2014;86:78-84.
27. Carretta A, Ciriaco P, Canneto B, Nicoletti R, Del Maschio A, Zannini P. Therapeutic strategy in patients with non-small cell lung cancer associated to satellite pulmonary nodules. *Eur J Cardiothorac Surg.* 2002;21:1100-1104.
28. Huang YH, Hsu KH, Tseng JS, Chen KC, Su KY, Chen HY, Chang CS, Chen JJ, Yu SL, Chen HW, Yang TY, Chang GC. Predilection of contralateral upper lung metastasis in upper lobe lung adenocarcinoma patients. *J Thorac Dis.* 2016;8:86-92.
29. Sánchez de Cos Escuin J, Abal Arca J, Melchor Íñiguez R, Miravet Sorribes L, Núñez Ares A, Hernández Hernández JR, García Arangüena L, Núñez Delgado M, Pavón Fernández MJ, Francisco Corral G, de Esteban Júlvez L, González Budiño MT, Abad Cavaco F, Ansótegui Barrera E, Andreo García F, Serra Mitjans M, Hernández Rodríguez H. Tumor, node and metastasis classification of lung cancer—M1a versus M1b—analysis of M descriptors and other prognostic factors. *Lung Cancer.* 2014;84:182-189.